Temporal changes of site response during the 2011 M_w 9.0 off the Pacific coast of Tohoku Earthquake

Chunquan Wu and Zhigang Peng

School of Earth and Atmospheric Sciences, Georgia Institute of Technology, Atlanta, GA 30332

(Received April 15, 2011; Revised June 7, 2011; Accepted June 8, 2011; Online published September 27, 2011)

The recent M_w 9.0 off the Pacific coast of Tohoku Earthquake and its aftershocks generated widespread strong shakings as large as ∼3000 Gal along the east coast of Japan. Here we systematically analyze temporal changes of material properties and nonlinear site response in the shallow crust associated with the Tohoku main shock, using seismic data recorded by the Japanese Strong Motion Network KiK-Net. We compute the spectral ratios of windowed records from a pair of surface and borehole stations, and then use the sliding-window spectral ratios to track the temporal changes in the site response of various sites at different levels of peak ground acceleration (PGA). Our preliminary results show clear drop of resonant frequency of up to 70% during the Tohoku main shock at 6 sites with PGA from 600 to 1300 Gal. In the site MYGH04 where two distinct groups of strong ground motions were recorded, the resonant frequency briefly recovers in between, and then followed by an apparent logarithmic recovery. We investigate the percentage drop of peak frequency and peak spectral ratio during the Tohoku main shock at different PGA levels, and find that at most sites they are correlated.

Key words: Tohoku Earthquake, earthquake ground motion, site effects, wave propagation, soil nonlinearity, KiK-Net.

1. Introduction

It is well known that local site conditions have significant effects on the strong ground motions generated during large earthquakes (e.g., Joyner *et al*., 1976; Chin and Aki, 1991; Yu *et al*., 1992). When the amplitude of ground motion exceeds a certain threshold, the sediment response deviates from the linear Hooke's law, resulting in nonlinear site effects (e.g., Beresnev and Wen, 1996a). The recent M_w 9.0 off the Pacific coast of Tohoku Earthquake on 03/11/2011 is the largest earthquake in Japan's long earthquake recording history. This great earthquake is recorded by ∼1200 K-NET/KiK-NET strong motion seismic stations with peak ground acceleration (PGA) at as high as ∼3000 Gal (Aoi *et al*., 2011). In addition, the long-duration (∼200 s) of the Tohoku Earthquake (Hayes *et al*., 2011) generate a wide range of ground motions between less than 10 Gal to more than 1000 Gal from the direct waves, followed by long coda waves. This provides an unprecedented dataset to quantify the degrees of nonlinear site response and the temporal changes over a wide range of PGA levels.

Previous measurements on nonlinear site response were mostly from PGAs in the range of a few tens of Gal to a few hundred Gal (e.g., Sawazaki *et al*., 2006; Wu *et al*., 2009a; Rubinstein, 2011). Their results are generally characterized by sharp reductions of the peak frequencies and peak spectral ratios during the large PGAs, followed by logarithmic recovery. In this short note we present preliminary results from temporal changes of site response associated with a wide range of PGAs during the Tohoku main shock.

2. Data and Analysis Procedure

2.1 Seismic data

The analysis employs strong motion data recorded by the Japanese Digital Strong-Motion Seismograph Network KiK-Net operated by National Research Institute for Earth Science and Disaster Prevention (Aoi *et al*., 2000). The network consists of 659 stations with an uphole/downhole pair of strong-motion seismometers. Each KiK-Net unit consists of three-component accelerometers and a data logger having a 24 bit analog-to-digital converter with a sampling frequency of 100 Hz. Additional details on the network and site conditions can be found at the KiK-Net website (http://www.kik.bosai.go.jp).

In this short note we analyze data recorded by six stations (FKSH10, IBRH12, IBRH15, IBRH16, MYGH04, TCGH16). The six stations generally feature strong velocity contrast between the surface soil layers and the underlying bedrocks. The soil layers at the top several tens of meters generally consist of clay, sandy clay, filling, and gravel with very low S-wave velocities of ∼100–200 m/s. The bedrocks are typically conglomerate, argillite, and shale with S-wave velocities of ∼700–3000 m/s. These stations are chosen mainly because the PGAs recorded are well above the common soil nonlinearity threshold of ∼200 Gal indicated by previous studies (Chin and Aki, 1991; Beresnev and Wen, 1996b), due to their relatively close distances to the epicenter of the Tohoku Earthquake. We also find that the observed temporal changes in peak frequencies and peak spectral ratios (maxima of the spectral

doi:10.5047/eps.2011.06.011

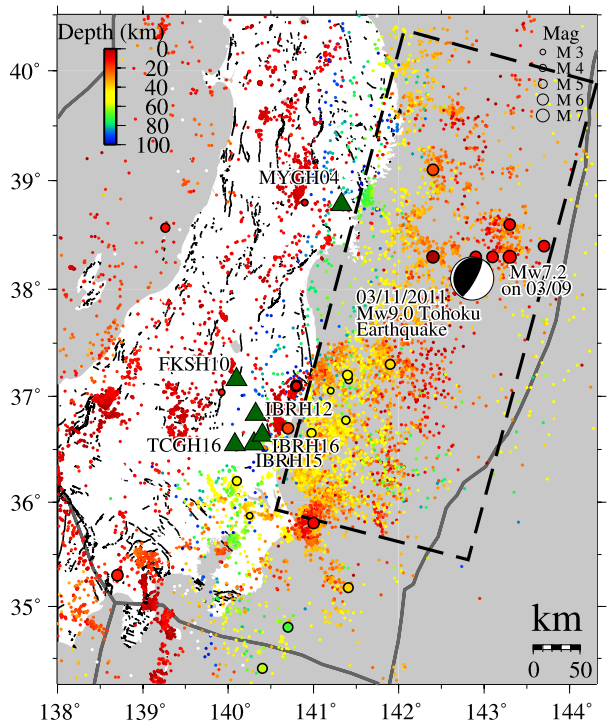

Fig. 1. Map of the study region in Japan. The epicenter of the 2011 M_w 9.0 Tohoku Earthquake is indicated by the moment tensor solution (beach ball symbol). The large, black rectangle represents the fault area of the 2011 Tohoku Earthquake, projected on the surface (Suzuki *et al.*, 2011). Epicenters of other events analyzed in this study are shown in large circles. The size of circle indicates the magnitude of each event and color shows the depth with red being shallow and blue being deep. The background events since 2011/01/01 from the Japan Meteorological Agency (JMA) catalog are shown as small dots. Locations of the 6 KiK-Net stations used in this study are shown in green triangles. The black lines show the active faults in this region and the grey lines denote the subduction plate boundaries.

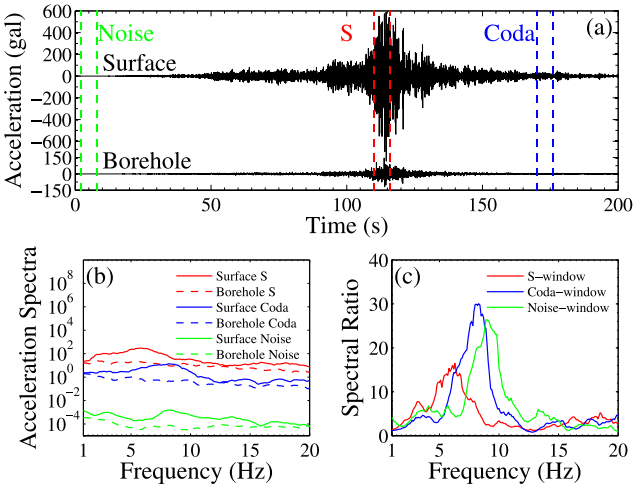

Fig. 2. (a) EW-component ground accelerations recorded at the station IBRH15 generated by the Tohoku main shock. Surface and borehole recordings are shown at the top and bottom panels, respectively. The green, red and blue dashed lines indicate the pre-event noise, direct *S* and coda window that are used to compute the acceleration spectra in (b) and spectral ratios in (c).

ratios) at these stations are much clearer than those at other stations, allowing us to better quantify temporal changes associated with the strong ground motion caused by the Tohoku main shock.

In the subsequent analysis we utilize a total of 32 events that occurred between 01/01/2011 and 03/28/2011 and recorded by the 6 surface and borehole strong motion sensors (Fig. 1). These include 22 events starting 73 days before, the Tohoku main shock, and 9 events within 17 days after the main shock. The magnitudes of the events range from 3 to 9, and the hypocentral depths range from 5 to 100 km. The maximum PGA recorded at these 6 stations is 1220 Gal.

2.2 Analysis procedure

The analysis procedure generally follows those of Sawazaki *et al.* (2006, 2009) and Wu *et al.* (2009a, b, 2010), and is briefly described here. We use 6-s time windows that are moved forward by 2 s for all waveforms recorded by the surface and borehole stations. All possible seismic phases, including pre-event noise, *P*, *S* and coda waves are analyzed together, and the PGA value is measured for each window. Note that here the term PGA refers to the maximum acceleration value in each window, rather than for the entire seismic records. We apply the sliding-window-based approach to the records of the Tohoku main shock to track the temporal changes during and immediately after the strong motion, and also to all the other events to measure the reference level of peak frequency and peak spectral ratio (see the Results section). Figure 2(a) shows an example of original acceleration records at station IBRH15 generated by the Tohoku main shock, the *S*-wave, coda wave, and pre-event noise windows used to compute the spectral ratio.

Next, we remove the mean value of the traces and apply a 5 per cent Hanning taper to both ends. We add the power spectra of the two horizontal components and take the square root of the sum to get the amplitude of the vector sum of the two horizontal spectra. The obtained spectra are smoothed by applying the mean smoothing algorithm from the subroutine "smooth" in the Seismic Analysis Code (Goldstein *et al.*, 2003), with half width of five points. The spectral ratio is obtained by taking the ratio of the horizontal spectra for surface and borehole stations. The amplitude of the spectra for both the surface and borehole recordings and the resulting spectral ratio at station IBRH15 are shown in Fig. 2(b) and (c).

3. Results

After processing all the data, we obtain 10272 spectral ratio traces for all the six stations from the sliding-window-based analysis. The running spectral ratios show clear decreases in peak spectral ratios and peak frequencies at the time of the Tohoku main shock, followed by an apparent logarithmic-type recovery (Fig. 3). In addition, for the station MYGH04, two bursts of strong ground motions were recorded, and the peak frequency briefly recovers in between, and then followed by an apparent logarithmic recovery (Fig. 3(d)).

To better quantify the temporal changes in site response associated with different levels of ground shaking, we sort the spectral ratios traces by their PGA values, and average them in PGA bins of every 10 Gal from 0 Gal to the

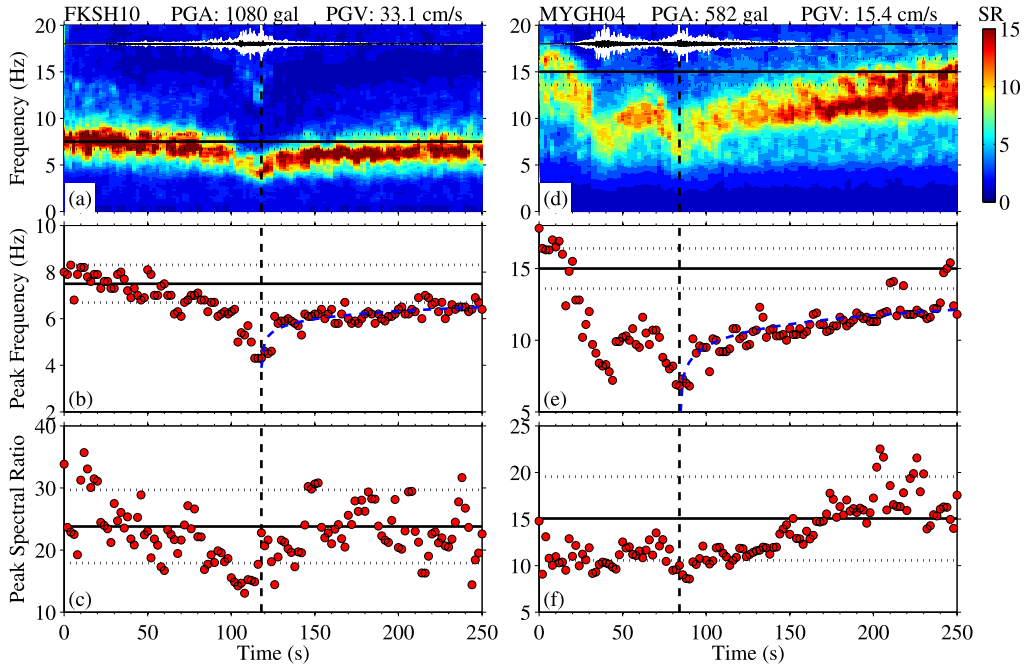

Fig. 3. (a) Color-coded surface/borehole spectral ratios plotted against time for the station FKSH10. The x-axis shows the time since the beginning of the recording, and the y-axis shows the frequency. The spectral ratio values are color-coded with red being high and blue being low. The vertical dashed lines indicate the time when the highest PGA value is recorded. The horizontal solid and dotted lines show the reference value and uncertainties of the peak frequency obtained by averaging all the spectral ratios for the windows before the P-arrivals of all the earthquakes between 2011/01/01 and 2011/03/28. The white and black traces on the top show the waveforms of the surface and borehole recordings, respectively. (b) Measured peak frequencies from (a). The horizontal and vertical lines are the same as in (a). The blue dashed curve shows the least-squares logarithmic fitting of the peak frequencies after the highest PGA. (c) Measured peak spectral ratios from (a). The horizontal solid and dotted lines show the reference value and uncertainties of the peak spectral ratio obtained by averaging all the spectral ratios for the windows before the P-arrivals of all the earthquakes between 2011/01/01 and 2011/03/28. (d–f) Similar plots as (a–c) for the station MYGH04.

maximum PGA level. We have tested changing the size of PGA bin from 1 Gal to 20 Gal, and the obtained results are similar. Next, we identify the peak spectral ratio and peak frequency of the stacked trace at each PGA bin, and then compute the percentage drop of peak frequency and peak spectral ratio (Fig. 4). The reference values of peak frequency and peak spectral ratio at each site are obtained by averaging all the spectral ratio traces for the windows before the P-arrivals of all the earthquakes at that site, assuming that the source and path effects are largely cancelled out by taking the spectral ratios between collocated surface and borehole stations. As shown in Fig. 2(c), the spectral ratio of the pre-event noise is very similar to the spectral ratio of the coda-window, except with a minor peak frequency shift. So this assumption is justified. We have tested averaging the spectral ratios of pre-event noise windows, coda windows, and direct S-arrival windows of small events as the reference spectral ratio, and the results are almost identical. According to Fig. 4, the percentage drop of peak frequency and peak spectral ratio range from 40–60% and 30–70%, respectively, and generally increase with the PGA level. We compute the first order polynomial (linear) least-squares fitting of the data in Fig. 4, and correlation coefficient is generally larger than 0.65. The only exception is the station TCGH16 where multiple peaks exist in the spectral ratios, which might introduce additional uncertainties in the measurement.

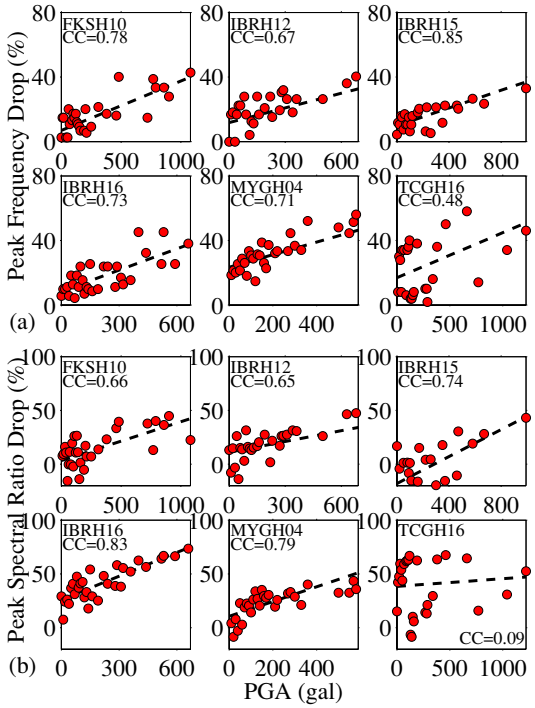

Fig. 4. (a) Calculated percentage drop of peak frequencies plotted against PGA at the six stations during the Tohoku main shock. The black dashed line shows the least-squares fitting of the data. Station names and correlation coefficient values are marked on the top-left corner of each panel. (b) Similar figure as (a) for the percentage drop of the peak spectral ratios.

4. Discussion

Previous studies have found clear evidences of soil nonlinearity after previous large earthquakes in Japan, including the 1995 M_w 6.8 Kobe earthquake, 2000 M_w 6.8 Western Tottori earthquake, 2003 M_w 8.3 Tokachi-Oki earthquake, 2003 M_w 7.0 Miyaki-Oki earthquake, and 2004 M_w 6.6 Niigata earthquake (e.g., Pavlenko and Irikura 2002; Sawazaki *et al*., 2006; Rubinstein *et al*., 2007; Assimaki *et al*., 2008; Wu *et al*., 2009a, 2010). The sharp reductions of the peak frequency and peak spectral ratio followed by gradual recovery observed in this study (Fig. 3) are similar to the previous observations of nonlinear site response using spectral ratio approaches (e.g., Sawazaki *et al*., 2006; Wu *et al*., 2009a). Hence, we attribute the temporal changes of the spectral ratios to nonlinear site response during the main shock.

Assuming a soft soil layer over a half-space bedrock with large impedance contrast (Dobry *et al*., 2000), the fundamental resonant frequency f of the soil layer can be computed by

$$f = \frac{V_s}{4H}, \tag{1}$$

where V_s and H are the S-wave velocity and thickness of the surface soil layer, respectively. Based on the site profiles of the 6 analyzed stations (see the KiK-Net website), strong velocity contrasts do occur between the surface sedimentary layers in the top several tens of meters and the underlying bedrock. The observed peak frequency in the spectral ratio traces (e.g., Fig. 3) generally matches the values computed from site profiles using Eq. (1). So the observed temporal changes are likely to be constrained within the surface sedimentary layers.

The peak frequency and peak spectral ratio generally recover to at least 90% of the reference value in time periods of several tens to several hundred seconds after the strong shaking (e.g., Fig. 3). At station MYGH04, the peak frequency drop to ∼45% of the reference value during the first phase, followed by a recovery to ∼80% of the reference value within ∼30 seconds. However, the recovery process is interrupted by a second phase, which is observed by many stations close the coast of Fukushima-Ibaraki (Aoi *et al*., 2011). The PGA of the secondary phase at MYGH04 is comparable to the first phase, and cause similar type of drop and recovery of the peak frequency and peak spectral ratio, with a recovery time scale of ∼150 seconds to the value before the second phase. We note that the peak frequency still do not recovery to the reference value at the end of the main shock record (∼250 s after the origin time). Whether this is due to permanent damage or longer time recovery remains to be investigated further with aftershock data. Due to the length of the available data at the time of writing, we are not able to look at the longer-period lower-amplitude temporal changes of the material properties as suggested by some previous studies (Lyakhovsky *et al*., 2009; Sawazaki *et al*., 2009).

As measured before, the percentage drop of peak frequency and peak spectral ratio measured during the Tohoku main shock correlate (with correlation coefficient larger than 0.65) with the PGA value at most sites (Fig. 4). The only exception is the station TCGH16, where there are two close peaks between 2 Hz and 6 Hz in the spectral ratio, which make the measurements of the peak frequency and peak spectral ratio more difficult and less accurate. The results in this study are generally consistent with the observation of Wu *et al*. (2009a) in the PGA range of 0 to ∼500 Gal, but extend the correlation between the soil nonlinearity and the input PGA to a much higher PGA range of 500 Gal to more than 1000 Gal. The slope between the input PGA and the degrees of nonlinearity varies at different sites, which is likely caused by different site conditions. We have checked the site profiles for the six stations from the KiK-Net website (http://www.kik.bosai.go.jp), including average S-wave velocity (V_{S30}) in the upper 30 m of the site (NEHRP 2003), soil types at the top layers of each site, and the S-wave velocity contrast. However we do not find clear correlation between the site conditions and observed degrees of nonlinearity.

In this short note we only focused on the clear temporal changes of site responses during the Tohoku main shock. Additional results on the long-term recovery and variable nonlinear behaviors will be reported in a follow-up work.

Acknowledgments. We thank National Research Institute for Earth Science and Disaster Prevention (NIED) for providing the KiK-net strong motion records of the 2011 Tohoku Earthquake sequence. We thank Joan Gomberg and an anonymous reviewer for their critical comments. This work is partially supported by National Science Foundation (EAR-0909310) and Southern California Earthquake Center (SCEC). SCEC is funded by NSF Cooperative Agreement EAR-0106924 and USGS Cooperative Agreement 02HQAG0008.

References

Aoi, S., K. Obara, S. Hori, K. Kasahara, and Y. Okada, New Japanese uphole/downhole strong-motion observation network: KiK-net, *Seismol. Res. Lett*, **72**, 239, 2000.

Aoi, S., T. Kunugi, W. Suzuki, N. Morikawa, H. Nakamura, N. Pulido, K. Shiomi, and H. Fujiwara, Strong motion characteristics of the 2011 Tohoku-oki earthquake from K-NET and KiK-NET, SSA Annual Meeting, 2011.

Assimaki, D., W. Li, J. Steidl, and K. Tsuda, Site amplification and attenuation via downhole array seismogram inversion: A comparative study of the 2003 Miyagi-Oki aftershock sequence, *Bull. Seismol. Soc. Am.*, **98**, 301–330, 2008.

Beresnev, I. and K. Wen, Nonlinear soil response—A reality?, *Bull. Seismol. Soc. Am.*, **86**, 1964–1978, 1996a.

Beresnev, I. and K. Wen, The possiblity of observing nonlinear path effect in earthquake-induced seismic wave propagation, *Bull. Seismol. Soc. Am.*, **86**, 1028–1041, 1996b.

Chin, B. and K. Aki, Simultaneous study of the source, path, and site effects on strong ground motion during the 1989 Loma Prieta earthquake: A preliminary result on pervasive nonlinear site effects, *Bull. Seismol. Soc. Am.*, **81**, 1859–1884, 1991.

Dobry, R., R. Borcherdt, C. Crouse, I. Idriss, W. Joyner, G. Martin, M. Power, E. Rinne, and R. Seed, New site coefficients and site classification system used in recent building seismic code provisions, *Earthquake Spectra*, **16**, 41–67, 2000.

Goldstein, P., D. Dodge, M. Firpo, and L. Minner, SAC2000: Signal processing and analysis tools for seismologists and engineers, in *In The IASPEI International Handbook of Earthquake and Engineering Seismology*, Part B, Chap 85.5, edited by Lee, W. H. K., H. Kanamori, P. C. Jennings, and C. Kisslinger, Academic Press, London, 2003.

Hayes, G., P. Earle, D. Wald, H. Benz, and R. Briggs, The USGS-NEIC response to the 2011/03/11 Mw9.0 Tohoku earthquake—magnitude and rupture modeling, SSA Annual Meeting, 2011.

Joyner, W., R. Warrick, and A. Oliver, Analysis of seismograms from a downhole array in sediments near San Francisco Bay, *Bull. Seismol. Soc. Am.*, **66**, 937–958, 1976.

Lyakhovsky, V., Y. Hamiel, J. Ampuero, and Y. Ben-Zion, Non-linear

damage rheology and wave resonance in rocks, *Geophys. J. Int.*, **178**, 910–920, 2009.

NEHRP, NEHRP recommended provisions for seismic regulations for new buildings and other structures (FEMA 450), National Earthquake Hazards Reduction Program (NEHRP), Building Seismic Safety Council, Washington, DC, 2003.

Pavlenko, O. and K. Irikura, Changes in shear moduli of liquefied and nonliquefied soils during the 1995 Kobe Earthquake and its aftershocks at three vertical-array sites, *Bull. Seismol. Soc. Am.*, **92**, 1952–1969, 2002.

Rubinstein, J., Nonlinear site response in medium magnitude earthquakes near Parkfield, California, *Bull. Seismol. Soc. Am.*, **101**, 275–286, 2011.

Rubinstein, J., N. Uchida, and G. Beroza, Seismic velocity reductions caused by the 2003 Tokachi-Oki earthquake, *J. Geophys. Res.*, B05315, 2007.

Sawazaki, K., H. Sato, H. Nakahara, and T. Nishimura, Temporal change in site response caused by earthquake strong motion as revealed from coda spectral ratio measurement, *Geophys. Res. Lett.*, **33**, L21303, doi:21310.21029/22006GL027938, 2006.

Sawazaki, K., H. Sato, H. Nakahara, and T. Nishimura, Time-lapse changes of seismic velocity in the shallow ground caused by strong ground motion shock of the 2000 Western-Tottori Earthquake, Japan, as revealed from coda deconvolution analysis, *Bull. Seismol. Soc. Am.*, **99**, 352–366, 2009.

Suzuki, W., S. Aoi, H. Sekiguchi, and T. Kunugi, Rupture process of the 2011 off the Pacific coast of Tohoku earthquake derived from strong-motion data, Japan Geoscience Union Meeting MIS036-P043, Makuhari, Chiba, Japan, May 022–027, 2011.

Wu, C., Z. Peng, and D. Assimaki, Temporal changes in site response associated with strong ground motion of 2004 Mw6.6 Mid-Niigata earthquake sequences in Japan, *Bull. Seismol. Soc. Am.*, **99**, 3487–3495, 2009a.

Wu, C., Z. Peng, and Y. Ben-Zion, Non-linearity and temporal changes of fault zone site response associated with strong ground motion, *Geophys. J. Int.*, **176**, 265–278, 2009b.

Wu, C., Z. Peng, and Y. Ben-Zion, Refined thresholds for nonlinear ground motion and temporal changes of site response associated with medium size earthquakes, *Geophys. J. Int.*, **183**, 1567–1576, doi:1510.1111/j.1365-1246X.2010.04704.x, 2010.

Yu, G., J. Anderson, and R. Siddharthan, On the characteristics of nonlinear soil response, *Bull. Seismol. Soc. Am.*, **83**, 218–244, 1992.

C. Wu (e-mail: chunquanwu@gatech.edu) and Z. Peng